

PAPER • OPEN ACCESS

## Controlling corrosion rate of Magnesium alloy using powder mixed electrical discharge machining

To cite this article: M A Razak *et al* 2018 *IOP Conf. Ser.: Mater. Sci. Eng.* **344** 012010

View the [article online](#) for updates and enhancements.

### Related content

- [XAFS analyses of zinc compound in corrosion product for magnesium alloy of super plastic processing](#)  
T Honma, H Mori, K Higashi et al.
- [A review on the effect of welding on the corrosion of magnesium alloys](#)  
N S Mohamed and J Alias
- [Anticorrosive magnesium hydroxide coating on AZ31 magnesium alloy by hydrothermal method](#)  
Yanying Zhu, Guangming Wu, Qing Zhao et al.

# Controlling corrosion rate of Magnesium alloy using powder mixed electrical discharge machining

M A Razak<sup>1,2</sup>, A M A Rani<sup>1,3</sup>, N M Saad<sup>3</sup>, G Littlefair<sup>4</sup> and A A Aliyu<sup>1,5</sup>

<sup>1</sup>Mechanical Engineering Department, Universiti Teknologi PETRONAS, Bandar Seri Iskandar, 32610, Perak, Malaysia

<sup>2</sup>Manufacturing Section, Universiti Kuala Lumpur Malaysian Spanish Institute, Kulim Hi-Tech Park, 09000, Kedah, Malaysia

<sup>3</sup>Biomedical Technology, Universiti Teknologi PETRONAS, Bandar Seri Iskandar, 32610, Perak, Malaysia

<sup>4</sup>School of Engineering, Faculty of Science, Engineering and Built Environment, Deakin University, Geelong, VIC 3220, Australia

<sup>5</sup>Department of Mechanical Engineering, Faculty of Engineering, Gwarzo Road, Bayero University Kano, Nigeria

Email: alhapis@unikl.edu.my

**Abstract.** Biomedical implant can be divided into permanent and temporary employment. The duration of a temporary implant applied to children and adult is different due to different bone healing rate among the children and adult. Magnesium and its alloys are compatible for the biodegradable implanting application. Nevertheless, it is difficult to control the degradation rate of magnesium alloy to suit the application on both the children and adult. Powder mixed electrical discharge machining (PM-EDM) method, a modified EDM process, has high capability to improve the EDM process efficiency and machined surface quality. The objective of this paper is to establish a formula to control the degradation rate of magnesium alloy using the PM-EDM method. The different corrosion rate of machined surface is hypothesized to be obtained by having different combinations of PM-EDM operation inputs. PM-EDM experiments are conducted using an opened-loop PM-EDM system and the in-vitro corrosion tests are carried out on the machined surface of each specimen. There are four operation inputs investigated in this study which are zinc powder concentration, peak current, pulse on-time and pulse off-time. The results indicate that zinc powder concentration is significantly affecting the response with 2 g/l of zinc powder concentration obtaining the lowest corrosion rate. The high localized temperature at the cutting zone in spark erosion process causes some of the zinc particles get deposited on the machined surface, hence improving the surface characteristics. The suspended zinc particles in the dielectric fluid have also improve the sparking efficiency and the uniformity of sparks distribution. From the statistical analysis, a formula was developed to control the corrosion rate of magnesium alloy within the range from 0.000183 mm/year to 0.001528 mm/year.

## 1. Introduction

The quality of an implant is important to determine the success of implantation [1]. Biomedical implant can be divided into permanent and temporary use. A temporary implant should allow sufficient duration for newly generated tissue to replace the bone defect [2-5]. A second surgery to



dissemble the temporary implant can be avoided by applying biodegradable implant [6]. Magnesium and its alloys have been established as being compatible for biodegradable implant [7-10]. Currently, the same type of implant is applied on both children and adult with only considering the difference in size. The real situation in the fractured bone healing process is that the different healing rate among the children and adult requires different corrosion rate of biodegradable implant. A temporary implant is normally applied to the children aged under six years for up to six months and adult for up to ten months [11-13]. However, it is difficult to control the degradation rate of magnesium alloy to be applied for children or adult biodegradable implant application. A method is required to control the degradation rate of magnesium alloy during the fabrication process. The objective of this paper is establishing a formula to control the degradation rate of magnesium alloy using the PM-EDM method. The different corrosion rate of machined surface was hypothesized to be obtained by having different combinations of PM-EDM operation inputs.

Machining magnesium alloy using conventional methods, such as milling, turning, and drilling, causes a built-up edge and chatter. The most important precaution needed to bear in mind whilst machining magnesium alloy is that the formation of fine chips and dust are highly flammable. The melting point of magnesium is 650°C, and this metal is only stable below its melting point. Non-traditional machining, such as the EDM process is preferable to machine magnesium based material, especially to machine the high geometrical accuracy required by bio-medical implants [14, 15].

Recently, new exploratory research works have been initiated to improve the efficiency of EDM process using PM-EDM method, a modified EDM process by adding powder in the dielectric fluid [16]. In PM-EDM, the added conductive particles help to improve the sparking efficiency during the ignition process. It was found that the addition of conductive particles as shown in Figure 1 led to increase the gap size between the tool electrode and the workpiece which subsequently ensuing in a reduction of the electrical discharge power density [17]. The added conductive particles have also lowered the dielectric strength, creating early and uniform electric discharges at low energy to improve the machined surface quality. In PM-EDM process, the added particles can be suspended in the dielectric fluid in the same machining tank or a separate tank. The use of a stirrer and circulating pump are to ensure the uniform distribution of the conductive particles [18-23].

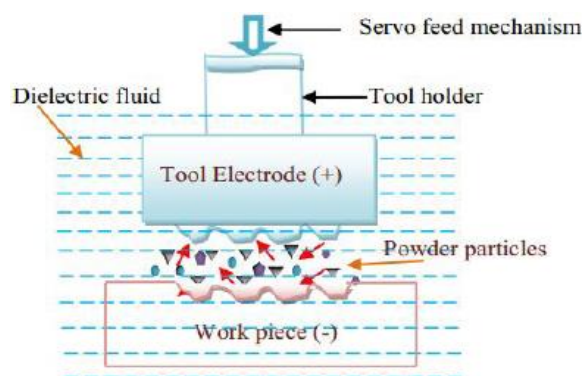


**Figure 1.** Electrical discharge during PM-EDM process [17].

Most of the researchers reported the advantages of PM-EDM in reducing the surface roughness, material removal rate, tool wear rate, and the modification of the machined surface [24-26]. For instance, it was found that the added titanium powder in the PM-EDM process on SKD61, SKD11, and SKT4 die steels improved the material removal rate by 42.1% as compared to conventional EDM (C-EDM) method [24]. On the other hand, it was suggested that some of the removed materials got deposited on the machined surface [27]. It was also reported that a significant decreased in surface crack density on the machined surface with silicon powder PM-EDM [28]. Figure 2 indicates a better surface quality obtained by the PM-EDM method compared to C-EDM method which possesses

several micro cracks. This phenomenon will result in reducing the metals' corrosion rate. Previously, an investigation indicates that the surface roughness of magnesium alloy processed using the PM-EDM method has been reduced by 44% [29]. However, there was no study have been done to investigate the effect of PM-EDM method on the corrosion rate of magnesium alloy. The advantages of the PM-EDM method deserve deeper clarification in order to meet the needs of high precision industries, such as the bio-medical and aerospace industries.

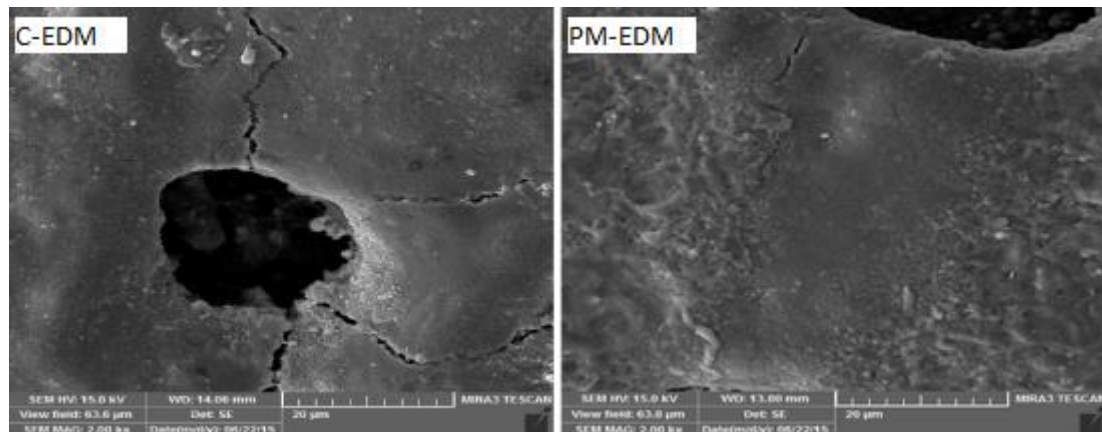


**Figure 2.** SEM micrographs of the machined surface by C-EDM and PM-EDM [30].

## 2. Materials and methods

PM-EDM experiments were conducted using Mitsubishi EA8 EDM die sinker with attached to opened-loop PM-EDM dielectric circulation system. The workpiece material used in this research was an AZ31 magnesium alloy and the tool electrode was copper. A constant cutting depth of 2 mm was maintained throughout the experiments. A preliminary experiment was conducted to determine the value range of the operation inputs. This research was conducted with four operation inputs as shown in Table 1. Each experiment was repeated diligently three times to ensure data accuracy. Zinc nanoparticles with an average size of 80 nm with three different concentrations were mixed in the dielectric fluid. Zinc was selected in this investigation due to the biocompatibility and it was one of the major components of the AZ31 magnesium alloy. Zinc is an effective alloying element for magnesium and can assist to improve its corrosion resistance [31]. By the deposition of zinc particles on the machined surface, the corrosion rate of magnesium alloy is hypothesized to be reduced significantly because the electrode potential of zinc (-0.76 V) is higher and more protected than magnesium (-2.37 V) [32].

**Table 1.** Experimental operation inputs.

Operation Input	Value
Zinc powder concentration	1, 2 and 3 g/l
Peak current	38, 47 and 55 A
Pulse on-time	16, 32 and 64 $\mu$ s
Pulse off-time	128, 256 and 512 $\mu$ s

The in-vitro corrosion tests were conducted with complying the ASTM G59-97 [33] and the simulated body fluid with components as shown in Table 2 were used. The corrosion rate of the machined surface was analyzed using the CH1608E electrochemical analyzer. Results from the corrosion test were analyzed using Design Expert software. Responses from the analysis of variance (ANOVA) were fitted into quadratic mathematical model.

**Table 2.** Hank's solution chemical composition [34].

Component	g/l
Sodium chloride, NaCl	8.00
Potassium chloride, KCl	0.40
Calcium chloride, CaCl <sub>2</sub>	0.14
Sodium bicarbonate, NaHCO <sub>3</sub>	0.35
Magnesium chloride hexahydrate, MgCl <sub>2</sub> .6H <sub>2</sub> O	0.60
Magnesium sulfate heptahydrate, MgSO <sub>4</sub> .7H <sub>2</sub> O	0.06
Sodium phosphate dibasic, Na <sub>2</sub> HPO <sub>4</sub>	0.06
Potassium phosphate monobasic, KH <sub>2</sub> PO <sub>4</sub>	0.60
Glucose.2H <sub>2</sub> O	1.0
pH	6.8

### 3. Results and discussion

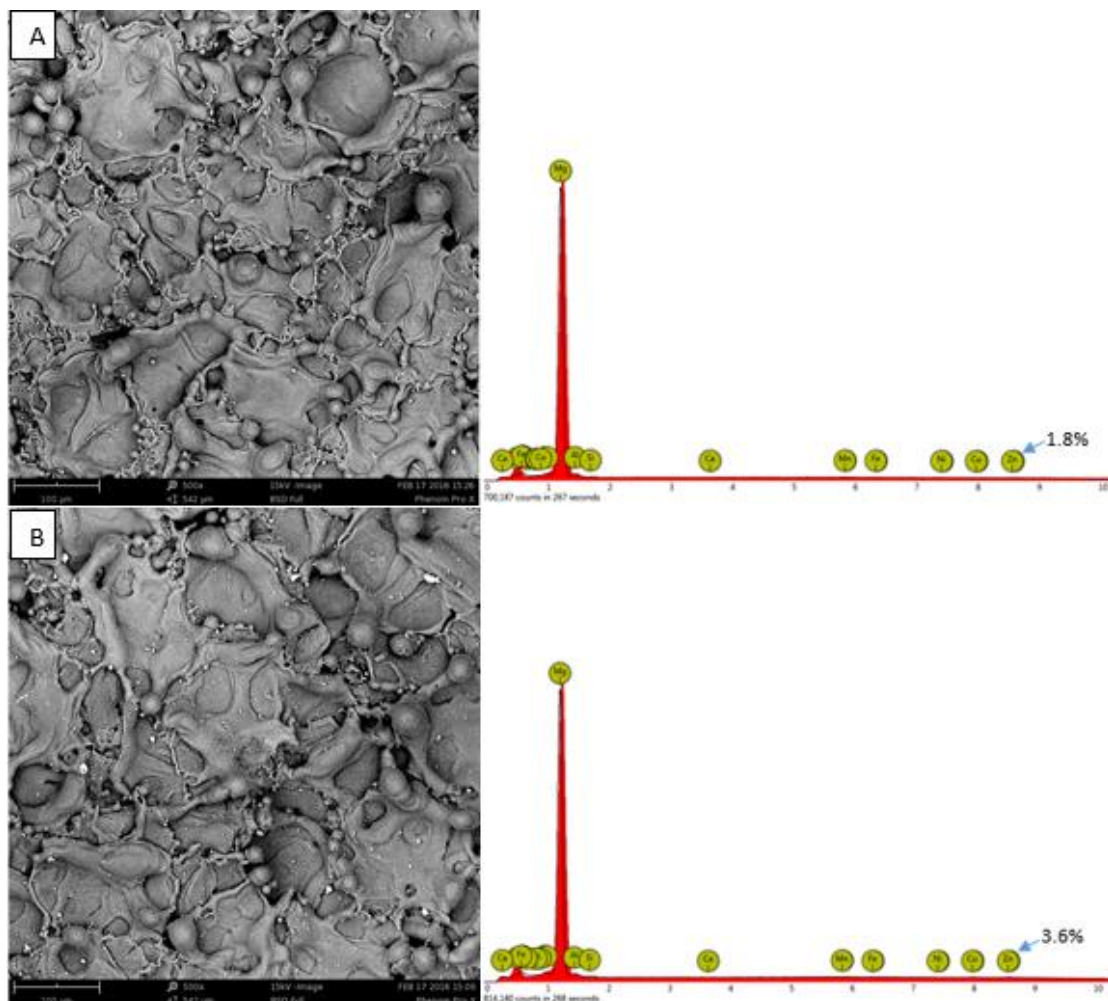


**Figure 3.** SEM images and EDX spectrum of magnesium alloy processed by; A) C-EDM method and B) PM-EDM method.

Initially, an experiment has been conducted using both C-EDM and PM-EDM method on the magnesium alloy specimen by applying the same operation inputs (47 A peak current, 80 V gap voltage, 16  $\mu\text{s}$  pulse on-time and 512  $\mu\text{s}$  pulse off-time). The objective was to evaluate the feasibility of the PM-EDM method in improving machined surface quality. The zinc particles with 1 g/l powder concentration were used in PM-EDM experiment. The surface roughness obtained from PM-EDM experiment was 4.971  $\mu\text{m}$ . The result shows a reduction of 10.61% surface roughness compared to C-EDM method (5.561  $\mu\text{m}$ ). The element composition analysis indicates that a higher weight percentage of zinc was found from the specimen processed by the PM-EDM method which was 1.8% higher than that from C-EDM method as presented in Figure 3. Some of the zinc particles mixed in the dielectric fluid get deposited on the machined surface during the experiment due to high localized temperature at the cutting zone. The suspended zinc particles in the dielectric fluid have also improve the sparking efficiency and the uniformity of sparks distribution [30].

The morphology disclosed from both machined surfaces was not much different. There were micro cracks, craters, globules and voids formed on both machined surfaces. From the corrosion test results as presented in Figure 4, it was found that the specimen processed by PM-EDM method obtained 24.15% lower corrosion rate than the specimen processed by C-EDM method. From this fact, the PM-EDM method seems promising to improve the machined surface quality and reduce the corrosion rate of magnesium alloy.

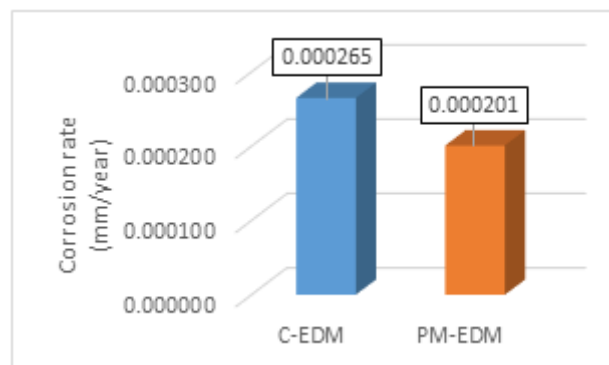


**Figure 4.** Corrosion rate of magnesium alloy processed by C-EDM and PM-EDM method.

Figure 5 presents the PM-EDM main effects plot of means with data response of means for corrosion rate. From the response table of means, pulse off-time with the delta value 0.000804 mm/year was identified as the most significant operation input affecting the changes of magnesium alloy corrosion rate. The results confirmed that the pulse off-time was inversely proportional to the response. The lower pulse off-time results in higher corrosion rate. The higher pulse off-time results in lower corrosion rate. This was due to the smoother machined surface obtained by the higher pulse off-time, hence obtaining the lower corrosion rate and vice versa. The zinc powder concentration with the delta value 0.000212 mm/year was also significantly affect the corrosion rate, which was more significant compared to peak current with the delta value 0.000172 mm/year and pulse on-time with the delta value 0.000157 mm/year. The presence of zinc particles in the dielectric fluid and high localized temperature at the cutting zone causes some zinc particles to get melted and deposited on the machined surface, hence improving the surface structure compared to the processed without zinc particles suspended in the dielectric fluid.

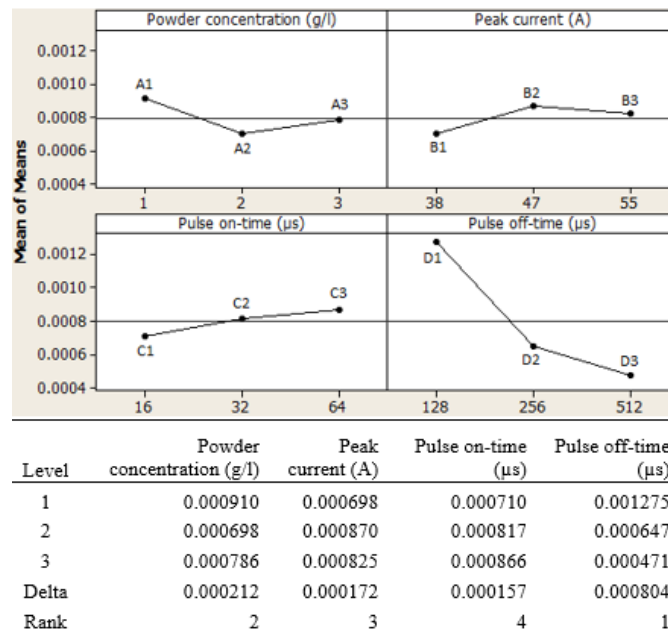


Figure 5. Main effects plot of means with data response of means for corrosion rate (mm/year).

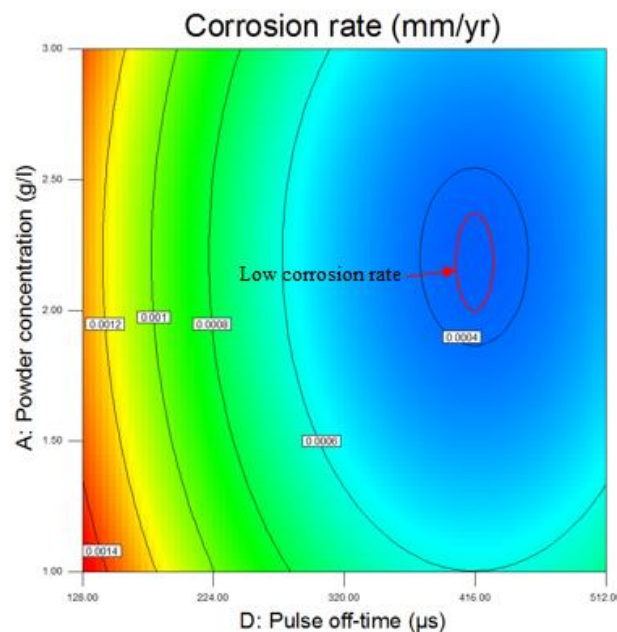


Figure 6. Interaction between zinc powder concentration and pulse off-time affects the corrosion rate of magnesium alloy.

Figure 6 presents the interaction between zinc powder concentration and pulse off-time affecting the corrosion rate of magnesium alloy machined surface processed by PM-EDM method. Within the range from 128 μs to 512 μs, the lowest corrosion rate has been obtained at 416 μs. Meanwhile, the highest corrosion rate was obtained at lowest pulse off-time, 128 μs. The higher pulse off-time applied in the EDM process contributing in better flushes of debris from the cutting area. A longer resting time allows the reduction of heat on the machined surface and the electrode. This phenomenon results in smoother machined surface with less formation of the cracks, craters and voids.

**Table 3.** ANOVA for response surface quadratic model.

Source	Sum of squares	df	Mean square	p-value
Model	3.51E-06	8	4.39E-07	< 0.0001
A-Zinc powder concentration	6.96E-08	1	6.96E-08	< 0.0001
B-Peak current	7.22E-08	1	7.22E-08	< 0.0001
C-Pulse on-time	1.1E-07	1	1.1E-07	< 0.0001
D-Pulse off-time	2.91E-06	1	2.91E-06	< 0.0001
A <sup>2</sup>	5.74E-08	1	5.74E-08	< 0.0001
B <sup>2</sup>	2.78E-08	1	2.78E-08	< 0.0001
C <sup>2</sup>	7.7E-09	1	7.7E-09	< 0.0001
D <sup>2</sup>	3.25E-07	1	3.25E-07	< 0.0001
Residual	2.09E-12	10	1.31E-13	
Cor Total	3.51E-06	24		

The interaction analysis reveals that there were interactions between all operation inputs during PM-EDM experiments. All four inputs were depending on each other in influencing the response. An interaction occurred when the effect of one input changes depending on the level of another input. It happened because the operation inputs determining the size of discharge energy. However, the ANOVA explicates that the interactions between two operation inputs were not significant affecting the machined surface corrosion rate since all the p-values for the interactions were more than 0.1. They were AB (zinc powder concentration with peak current), AC (zinc powder concentration with pulse on-time), AD (zinc powder concentration with pulse off-time), BC (peak current with pulse on-time), BD (peak current with pulse off-time) and CD (pulse on-time with pulse off-time). Therefore, these measurements were withdrawn from the ANOVA reduced quadratic analysis as presented in Table 3 to obtain the formula on PM-EDM operation inputs to control the corrosion rate of magnesium alloy. The model has eight degrees of freedom and total correlations of 24 degrees of freedom. The determined constants for final equation in terms of actual factors are:

$$\begin{aligned} \text{Corrosion rate} &= -7.81276 \times 10^{-4} \\ \text{Zinc powder concentration} &= -6.62901 \times 10^{-4} \\ \text{Peak current} &= 1.42548 \times 10^{-4} \\ \text{Pulse on-time} &= 1.19244 \times 10^{-5} \\ \text{Pulse off-time} &= -9.13054 \times 10^{-6} \\ \text{Squared zinc powder concentration} &= 1.50184 \times 10^{-4} \\ \text{Squared peak current} &= -1.45265 \times 10^{-6} \\ \text{Squared pulse on-time} &= -1.08257 \times 10^{-7} \\ \text{Squared pulse off-time} &= 1.09936 \times 10^{-8} \end{aligned}$$

The quadratic mathematical model is given as equation (1). The formula has been elaborated and the final formula is shown in equation (2) where *CR* is the corrosion rate, *W* is the zinc powder concentration, *X* is the peak current, *Y* is the pulse on-time and *Z* is the pulse off-time.



$$CR = \beta_0 + \beta_W W + \beta_X X + \beta_Y Y + \beta_Z Z + \beta_{WW} W^2 + \beta_{XX} X^2 + \beta_{YY} Y^2 + \beta_{ZZ} Z^2 \quad (1)$$

$$CR = (-7.81276 \times 10^{-4}) + (-6.62901 \times 10^{-4})W + (1.42548 \times 10^{-4})X + (1.19244 \times 10^{-5})Y \\ + (-9.13054 \times 10^{-6})Z + (1.50184 \times 10^{-4})W^2 + (-1.45265 \times 10^{-6})X^2 \\ + (-1.08257 \times 10^{-7})Y^2 + (1.09936 \times 10^{-8})Z^2 \quad (2)$$

With the established formula, the corrosion rate of magnesium alloy can be forecasted by changing the values of PM-EDM operation inputs as long as the values are within the limits. The range of values for each operation inputs are:

- Zinc powder concentration: 1 g/l to 3 g/l
- Peak current: 38 A to 55 A
- Pulse on-time: 16  $\mu$ s to 64  $\mu$ s
- Pulse off-time: 128  $\mu$ s to 512  $\mu$ s

The lowest corrosion rate computed by this formula is 0.000183 mm/year from the combination of 2 g/l zinc powder concentration, 38 A peak current, 16  $\mu$ s pulse on-time and 512  $\mu$ s pulse off-time. Meanwhile, the highest corrosion rate computed by this formula is 0.001528 mm/year from the combination of 1 g/l zinc powder concentration, 47 A peak current, 64  $\mu$ s pulse on-time and 128  $\mu$ s pulse off-time. To verify the formula, a confirmation test was conducted by applying the combination of 1 g/l zinc powder concentration, 38 A peak current, 16  $\mu$ s pulse on-time and 128  $\mu$ s pulse off-time. The predicted value was 0.0012 mm/year and the actual value was 0.0013 mm/year. It brought to 91.67% similarity between the predicted and actual values.

#### 4. Conclusions

It can be concluded that the pulse off-time was the most significant operation input affecting the corrosion rate of magnesium alloy with the higher pulse off-time ensuing in lower corrosion rate. The zinc particles mixed in the dielectric fluid was also found significantly affecting the changes of the corrosion rate of magnesium alloy. Among the three levels of zinc powder concentration examined, the 2 g/l zinc powder concentration obtained the lowest corrosion rate. The different combination of PM-EDM operation inputs was found results in different surface characteristics on the machined surfaces hence resulting in different corrosion rate. The presence of zinc particles at the cutting zone contribute into improving sparking efficiency and uniformity of sparks distribution. The deposition of zinc particles on the machined surface results in lower smoother machined surface with less formation of micro cracks. These factors influencing the changes of corrosion rate on the machined surface. With the developed formula, the corrosion rate of magnesium alloy can be controlled by controlling PM-EDM operation inputs. For future investigation, it is recommended to conduct in-vivo corrosion test using an implant processed by PM-EDM method.

#### References

- [1] M. Genisa, Z. A. Rajion, D. Mohamad, A. Pohchi, M. R. A. Kadir, and S. Shuib, "Effect of Different Angle Scanning on Density Estimation Based on Hounsfield Unit on CT and CBCT," *Sains Malaysiana*, vol. 44, pp. 1331-1337, 2015.
- [2] H. Park, J. S. Temenoff, and A. G. Mikos, "Biodegradable orthopedic implants," in *Engineering of Functional Skeletal Tissues*, ed: Springer, 2007, pp. 55-68.
- [3] L. Nassif and M. El Sabban, "Mesenchymal stem cells in combination with scaffolds for bone tissue engineering," *Materials*, vol. 4, pp. 1793-1804, 2011.
- [4] J. L. Olson, A. Atala, and J. J. Yoo, "Tissue engineering: current strategies and future directions," *Chonnam Medical Journal*, vol. 47, pp. 1-13, 2011.
- [5] J. S. Temenoff and A. G. Mikos, "Injectable biodegradable materials for orthopedic tissue engineering," *Biomaterials*, vol. 21, pp. 2405-2412, 2000.

- [6] P. H. Long, "Medical devices in orthopedic applications," *Toxicologic Pathology*, vol. 36, pp. 85-91, 2008.
- [7] M. T. Andani, N. S. Moghaddam, C. Haberland, D. Dean, M. J. Miller, and M. Elahinia, "Metals for bone implants. Part 1. Powder metallurgy and implant rendering," *Acta Biomaterialia*, vol. 10, pp. 4058-4070, 2014.
- [8] P. R. Cha, H. S. Han, G. F. Yang, Y. C. Kim, K. H. Hong, S. C. Lee, *et al.*, "Biodegradability engineering of biodegradable Mg alloys: Tailoring the electrochemical properties and microstructure of constituent phases," *Scientific Reports*, vol. 3, pp. 1-6, 2013.
- [9] F. Witte, "The history of biodegradable magnesium implants: a review," *Acta Biomaterialia*, vol. 6, pp. 1680-1692, 2010.
- [10] S. Zhang, X. Zhang, C. Zhao, J. Li, Y. Song, C. Xie, *et al.*, "Research on an Mg-Zn alloy as a degradable biomaterial," *Acta Biomaterialia*, vol. 6, pp. 626-640, 2010.
- [11] O. Islam, D. Soboleski, S. Symons, L. Davidson, M. Ashworth, and P. Babyn, "Development and duration of radiographic signs of bone healing in children," *American Journal of Roentgenology*, vol. 175, pp. 75-78, 2000.
- [12] W. Jackson, T. Theologis, C. Gibbons, S. Mathews, and G. Kambouroglou, "Early management of pathological fractures in children," *Injury*, vol. 38, pp. 194-200, 2007.
- [13] P. V. Giannoudis, E. Jones, and T. A. Einhorn, "Fracture healing and bone repair," *Injury*, vol. 42, pp. 549-550, 2011.
- [14] F. Klocke, M. Schwade, A. Klink, and A. Kopp, "EDM machining capabilities of Magnesium (Mg) alloy WE43 for medical applications," *Procedia Engineering*, vol. 19, pp. 190-195, 2011.
- [15] M. A. Razak, A. M. Abdul-Rani, T. V. V. L. N. Rao, S. R. Pedapati, and S. Kamal, "Electrical discharge machining on biodegradable AZ31 magnesium alloy using Taguchi method," *Procedia Engineering*, vol. 148, pp. 916-922, 2016.
- [16] A. Singh and R. Singh, "Effect of powder mixed electric discharge machining (PMEDM) on various materials with different powders: A review," *International Journal for Innovative Research in Science and Technology*, vol. 2, pp. 164-169, 2015.
- [17] M. A. Tawfiq and A. S. Hameed, "Effect of powder concentration in PMEDM on surface roughness for different die steel types," *International Journal of Current Engineering and Technology*, vol. 5, pp. 3323-3329, 2015.
- [18] H. Kansal, S. Singh, and P. Kumar, "Technology and research developments in powder mixed electric discharge machining (PMEDM)," *Journal of Materials Processing Technology*, vol. 184, pp. 32-41, 2007.
- [19] S. Mohal, H. Kumar, and S. Kansal, "Nano-finishing of materials by powder mixed electric discharge machining (PMEDM): A review," *Science of Advanced Materials*, vol. 7, pp. 2234-2255, 2015.
- [20] A. M. Nanimina, A. M. A. Rani, and T. L. Ginta, "Assessment of powder mixed EDM: A review," in *MATEC Web of Conferences*, 2014, p. 04018.
- [21] S. Kumar and U. Batra, "Surface modification of die steel materials by EDM method using tungsten powder-mixed dielectric," *Journal of Manufacturing Processes*, vol. 14, pp. 35-40, 2012.
- [22] M. A. Razak, A. M. Abdul-Rani, and A. M. Nanimina, "Improving EDM efficiency with silicon carbide powder-mixed dielectric fluid," *International Journal of Materials, Mechanics and Manufacturing*, vol. 3, pp. 40-43, 2015.
- [23] Y. F. Tzeng and C. Y. Lee, "Effects of powder characteristics on electrodischarge machining efficiency," *The International Journal of Advanced Manufacturing Technology*, vol. 17, pp. 586-592, 2001.
- [24] B. T. Long, N. H. Phan, N. Cuong, and V. S. Jatti, "Optimization of PMEDM process parameter for maximizing material removal rate by Taguchi's method," *The International Journal of Advanced Manufacturing Technology*, pp. 1-11, 2016.

- [25] A. Bhattacharya, A. Batish, and N. Kumar, "Surface characterization and material migration during surface modification of die steels with silicon, graphite and tungsten powder in EDM process," *Journal of Mechanical Science and Technology*, vol. 27, pp. 133-140, 2013.
- [26] P. Janmanee, "Performance of Cu-Cr-Zr electrodes in electrical discharge machining of tungsten carbide composite material base using Taguchi method," *International Journal of Machining and Machinability of Materials*, vol. 18, pp. 412-425, 2016.
- [27] A. Batish and A. Bhattacharya, "Mechanism of material deposition from powder, electrode and dielectric for surface modification of H11 and H13 die steels in EDM process," *Materials Science Forum*, vol. 701, pp. 61-75, 2012.
- [28] C. Prakash, H. Kansal, B. Pabla, and S. Puri, "Experimental investigations in powder mixed electric discharge machining of Ti-35Nb-7Ta-5Zr $\beta$ -titanium alloy," *Materials and Manufacturing Processes*, pp. 1-13, 2016.
- [29] A. Abdul-Rani, M. Razak, G. Littlefair, I. Gibson, and A. Nanimina, "Improving EDM Process on AZ31 Magnesium Alloy towards Sustainable Biodegradable Implant Manufacturing," *Procedia Manufacturing*, vol. 7, pp. 504-509, 2016.
- [30] M. Shabgard and B. Khosrozadeh, "Investigation of carbon nanotube added dielectric on the surface characteristics and machining performance of Ti-6Al-4V alloy in EDM process," *Journal of Manufacturing Processes*, vol. 25, pp. 212-219, 2017.
- [31] M. M. Avedesian and H. Baker, *ASM specialty handbook: magnesium and magnesium alloys*: ASM international, 1999.
- [32] R. K. Rajput, *Material Science and Engineering*, 3rd ed. New Delhi: S.K. Kataria & Sons, 2012.
- [33] A. Standard, "G59-97: Standard Test Method for Conducting Potentiodynamic Polarization Resistance Measurements," *West Conshohocken, PA: ASTM International*, 2009.
- [34] A. R. H. Bidhendi and M. Pouranvari, "Corrosion study of metallic biomaterials in simulated body fluid," *Metalurgija*, vol. 17, pp. 13-22, 2011.